

On Coupling with EMI Capacitors

Stefan-Peter Weber, Eckart Hoene, Stephan Guttowski, Werner John, Herbert Reichl
Fraunhofer Institute for Reliability and Microintegration
Gustav-Meyer-Allee 25, 13355 Berlin, Germany
Email: stefan-peter.weber@izm.fraunhofer.de

Abstract—So far, methodical design of EMI filters for power electronic applications fails, because coupling among the filters' components is not predicted accurately. In this paper a calculation method of coupling with EMI capacitors is presented. The method is verified by experimental results. The presented results prove the possibility of simulating field coupling in circuits including the circuit's components. In particular when miniaturizing power electronic devices the calculated coupling among conductors and components must be taken into account to ensure EMC at the system level.

I. INTRODUCTION

So far, the radio frequency behaviour of EMI filters for power electronic applications is not considered during the design phase [1], [2]. In EMI filters, where clean lines exist next to noise carrying lines and components, very small coupling coefficients have a significant influence on the filter's insertion loss [3]. In particular when miniaturizing power electronic devices the coupling among conductors and components must be taken into account to ensure EMC at the system level.

State of the art in modeling coupling paths in power electronic systems is the quasi-static evaluation of conducting materials by the Partial Elements Equivalent Circuit (PEEC) method [4]. The PEEC method was presented in 1974 by Ruehli [5] and is now available in a number of software tools.

In this paper a modeling method for coupling with EMI capacitors is presented. The method is verified by experimental results. The presented results prove the possibility of simulating field coupling in circuits including the circuit's components.

In this paper it is proven that components like capacitors can be included in the system simulation as well as conductors between the components. Parasitic inductances of EMI capacitors and mutual magnetic and capacitive coupling is calculated on the basis of the geometry. Both, the capacitor's impedance and its coupling to near conductors, are predicted. Accuracy of the calculations is verified by experimental results in the frequency range from some kHz up to 100 MHz.

II. CAPACITORS UNDER TEST

For the design of EMI filters in power electronic applications, EMI capacitors usually range from 10nF up to 5 μ F for voltages about 300V. For the investigation of coupling with an EMI capacitor, a 100nF, a 330nF and a 1 μ F capacitor are chosen. Figure 1 shows the impedance of the three capacitors in the regarded frequency range from 1kHz up to 100MHz. The capacitance value is highly accurate up to a first resonance frequency f_r at a few MHz. After

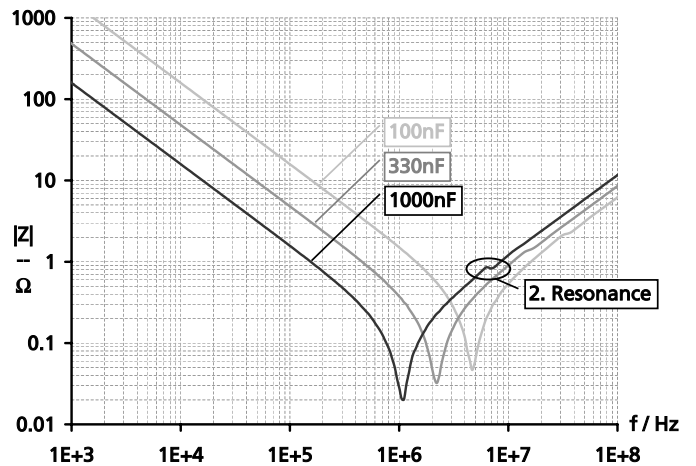


Fig. 1. Impedance of tested capacitors

that resonance frequency f_r the capacitor behaves like an inductor. A second resonance occurs at higher frequencies due to a floating electrode increasing the proof voltage [6]. The variation of impedance at the second resonance is small for the tested capacitors and therefore not further stressed in this paper. The measurement presented in Figure 1 delivers a low

TABLE I
EQUIVALENT SERIES RESISTANCES (ESR)

Capacitance in nF	ESR in m Ω
100	38
330	29
1004	20

Equivalent Series Inductance (ESL) depending on the length of the capacitors' connectors to the impedance analyzer. Thus the ESL of a capacitor connected in a circuit must be determined taking into account the whole loop of the capacitor connectors. From the impedance measurement of a single capacitor the Equivalent Series Resistance (ESR) and the capacitance value itself can be obtained and are listed in Table I.

III. EXPERIMENTAL SETUP

For the determination of coupling with EMI capacitors an antenna loop is placed close to a capacitor. Induced voltage is measured related to the voltage at the capacitor's connectors by a Gain-Phase-Analyzer in the regarded frequency range from some kHz up to 100MHz. The induced voltage strongly

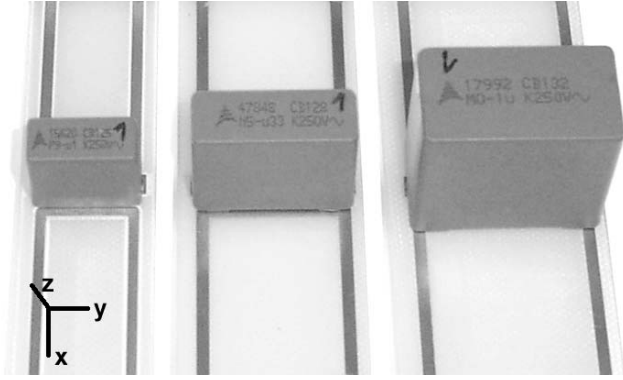


Fig. 2. Experimental setups with different grid size

depends on the distance between the loop with the capacitor and the antenna loop. The chosen measurement setup provides distinct values wherever the antenna loop is placed in all three dimensions but close (within a distance of 10cm) to the loop with the capacitor. In Section VI the influence of the position of the antenna loop is discussed and the possibility to predict it is proven. At first coupling is analyzed for an antenna loop on the same level with the capacitor's connectors. The chosen capacitors have typical grid sizes of 15mm, 22.5mm and 27.5mm. The grid scales with the capacitance value. Figure 2 shows the setups for the evaluation of received voltage at capacitors with three different grid sizes.

IV. MUTUAL MAGNETIC COUPLING

A. Equivalent Circuit

Mutual magnetic coupling is supposed to be dominant because of the setups' size. The experimental setup is firstly modeled by the equivalent circuit shown in Figure 3. R_1 is the resistance of the loop connecting the capacitor, modeled by C, ESR and ESL, a common series resonance circuit. The secondary side of the coupled system is the antenna loop: R_2 is the resistance and L_2 the self-inductance of the antenna loop connected to 50Ω -input of the Gain-Phase Analyzer. M identifies mutual magnetic coupling between both loops. The current I_1 in the loop with the capacitor increases with the frequency as the impedance of the capacitor decreases until the resonance frequency at about 1MHz. At higher frequencies I_1

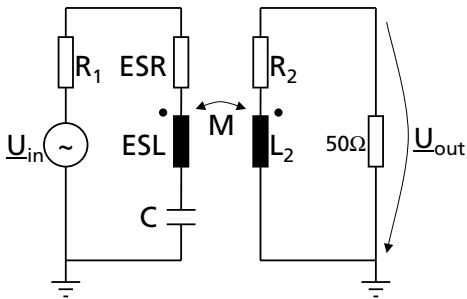


Fig. 3. Equivalent circuit of the measurement setup

decreases due to the inductive impedance of the loop with the capacitor. The induced voltage at the antenna loop is proportional to the frequency and to the current in the loop with the capacitor.

$$Gain = \frac{U_{out}}{U_{in}} \quad (1)$$

$$= \frac{j\omega M I_1 - (R_2 + j\omega L_2) I_2}{(R_1 + ESR + j\omega ESL - j\frac{1}{\omega C}) I_1 + j\omega M I_2}$$

$$\approx \frac{j\omega M}{R_1 + ESR + j\omega ESL - j\frac{1}{\omega C}} \text{ as } I_2 \ll I_1$$

$$|Gain| \approx \omega^2 \frac{M}{C} \sim f^2 \quad \text{for } f < f_r \quad (2)$$

$$|Gain| \approx \frac{M}{ESL} = const. \quad \text{for } f > f_r \quad (3)$$

As R_2 's and L_2 's Impedance is small compared to 50Ω and there is no backlash (as $I_2 \ll I_1$), the Gain to be measured yields approximately Equations 2 and 3 for frequencies beneath and above the resonance frequency f_r .

B. Test Results

Figure 4 shows the measured voltage at the antenna loop related to the voltage at the loop with the capacitor in dB. Values below -80dB are not displayed because very low values can not be measured accurately. At frequencies below the resonance frequency the measured voltage rises with f^2 (40dB/decade) as expected (Equation 2). After the resonance frequency the capacitor's current decreases due to the inductive impedance of the loop with the capacitor, but as the induced voltage is proportional to the frequency and the current, it remains constant (Equation 3). Assuming self and mutual inductances approximately proportional to the loop area, higher induced voltage is expected with larger capacitors and therefore larger grids. This is not the case as can be seen at frequencies higher than the resonance frequency. As expected, coupling from the loop with the 330nF capacitor is higher than from the loop with the smaller 100nF capacitor. But

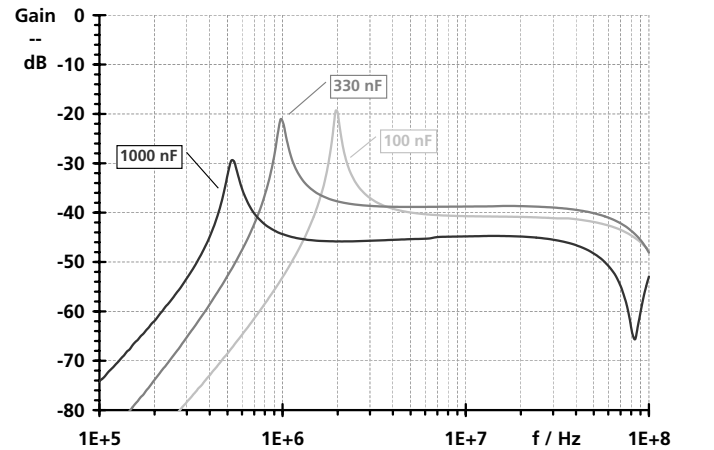


Fig. 4. Measured gain with different grid size

coupling from the loop with a $1\mu\text{F}$ capacitor is much lower. Thus, the shape of the component itself must have a significant influence on the coupling behaviour. The setup with the $1\mu\text{F}$ capacitor shows a second resonance frequency at the end of the regarded frequency range due to mutual capacitive coupling. Capacitive coupling is not negligible when taking into account the components' coupling at the system level and is therefore discussed in Section V.

C. Limits for Reachable Modeling Accuracy

In the following a method is presented for calculating the parameters of the equivalent circuit in Figure 3. Another experiment clearly shows the limits for the accuracy of such calculations. The different coupling behaviour of a capacitor and the same component rotated 180° is in the same range of $\pm 2\text{dB}$ like the difference between different exemplars of a capacitor. Figure 5 shows this experiment with the $1\mu\text{F}$ capa-

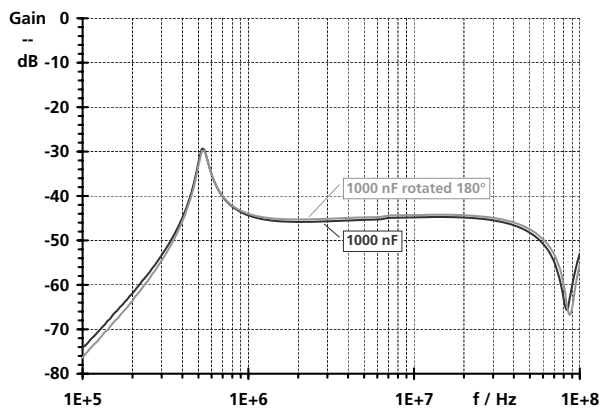


Fig. 5. Measured gain with $1\mu\text{F}$ capacitor and the same capacitor rotated 180°

capitor. The different coupling behaviour of exemplars and even the same component rotated 180° is owed by tolerances of the position of the metalized film roll building the capacitance within the capacitor's housing. The metalized film roll is the radio-frequency current carrying part of the component and therefore its geometry and position is responsible not only for capacitance but also for inductance and coupling behaviour. In order to calculate the model parameters the geometry of metalized film rolls has to be known.

D. Geometry of Metalized Film Rolls

The geometry of metalized film rolls of EMI capacitors is usually not given in the datasheet by the manufacturer. Thus six exemplars of each capacitor are cut. Three exemplars are cut for a cross section through the connectors (yz -level) and three are cut for a cross section perpendicular (xz -level). The geometry is measured with an appropriate microscope. The values of interest are the dimensions of the roll and its position within its housing. The cross section in the xz -level is described by the roll's width, height and the corner radius. The cross section in the yz -level provides information

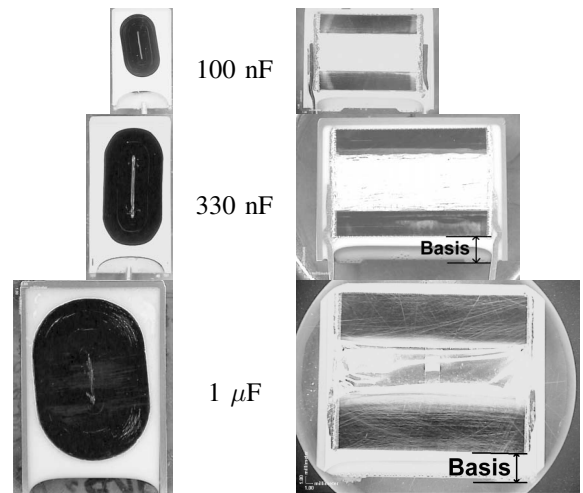


Fig. 6. Geometry of metalized film rolls: xz -level on the left, yz -level on the right

TABLE II
DIMENSIONS OF METALIZED FILM ROLLS IN MM

Capacitor	x: width	y: length	z: height	radius	basis
100 nF	4.6	14.9	8.6	2.3	2.7
330 nF	7.4	24.1	15.0	3.7	4.0
$1\mu\text{F}$	17.1	28.6	24.6	8.5	4.5

about the rolls length and the distance between the level of the connectors and the bottom edge of the roll ("basis" in the following). As differences between exemplars are not to be modeled only the basis is measured, assuming the roll is placed vertically and centered within its housing. The cross sections in Figure 6 clearly show big discrepancies of the positions of the rolls with this assumption. While for the 330nF capacitor a straight exemplar close to the center is shown, the $1\mu\text{F}$ capacitor is placed lopsided. The exemplar of the 100nF seems to be squeezed towards the top of its housing. Thus the difference in coupling behaviour of one component rotated 180° shown in Figure 5 becomes understandable. It is obvious that a component with a right sided position of the roll couples more with an antenna loop placed on the right side than if it was rotated 180° . Let's have a look on Figure 5: At frequencies lower than the resonance coupling is lower with the component rotated 180° , as expected for a right sided roll. At frequencies higher than the resonance the coupling is higher with the component rotated 180° ! What we see here results from a lopsided roll and the proximity effect. With higher frequencies the radio frequency current distributes more towards its return conductor. Thus, in the lopsided component the current flows at lower frequencies with more distance to the antenna loop than at high frequencies, where it becomes torn towards its return. These effects clearly show the limits in modeling accuracy. In the following metalized film rolls are considered to be placed straight and centered. Frequency dependency of the coupling parameters is neglected. Average values of the obtained dimensions are listed in Table II.

E. Modeling

The test setup is modeled for the determination of the parameters of the equivalent circuit shown in Figure 3 by the PEEC method. Conducting materials are discretized in cuboid conducting elements for the calculation of resistances and partial and mutual inductances between all elements [4], [5]. Loop inductances are then calculated by adding the signed partial inductances of the loops. In order to properly model non-uniform cross sectional current distribution due to diffusion the cuboid elements can be further discretized in more filaments. Resistances and inductances are determined from DC to 100 MHz. Values at 1 MHz are chosen for the parameters of the equivalent circuit in order to obtain a model valid in frequency and time domain. Rising resistances due to skin effect are small compared to ESR and 50Ω . Loss of inner inductance due to skin effect is negligible. Dependency on the frequency of mutual inductances due to non-uniform current distribution is supposed to be small as well. Dependency on the frequency of all the model parameters is small and therefore unattended.

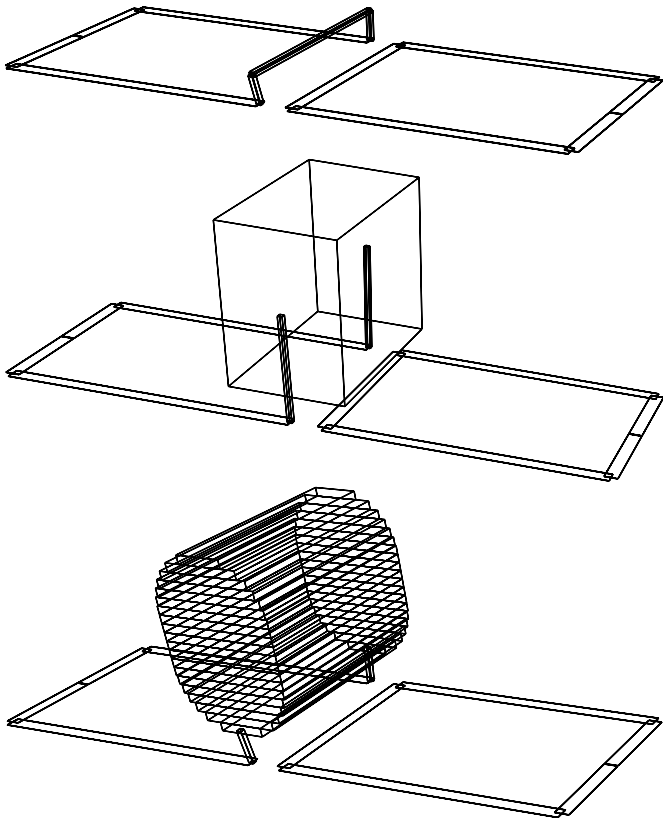


Fig. 7. Modeling approaches: proximity assumption, cuboid and 80 elements shaping the metalized film roll of the $1\mu\text{F}$ capacitor

The conductors of the antenna loop and the connector loop for the capacitances are $35\mu\text{m}$ thick and 2mm wide traces on printed circuit boards (PCB). Because of their rectangular cross section they are exactly modeled by PEEC elements. The wires connecting the metalized film roll to the PCB are round

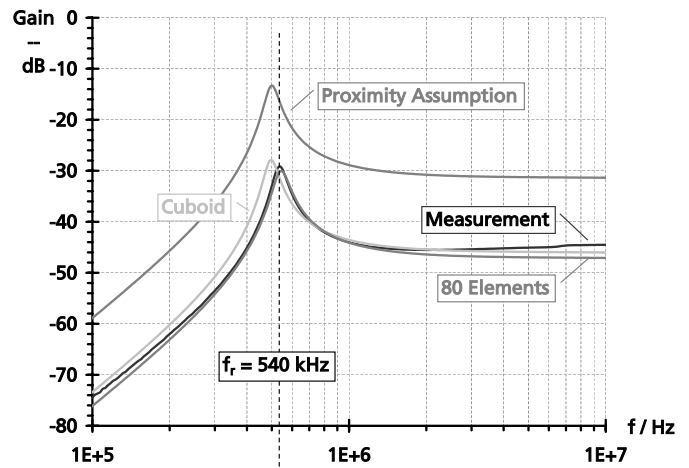


Fig. 8. Different discretization of the metalized film roll of the $1\mu\text{F}$ capacitor

with a diameter of 0.8mm. Goerisch [4] proved that partial self and mutual inductances of round conductors can be accurately determined using square PEEC elements with edges of length .8725 times the diameter. There is no mistake for the partial self inductance and deviation in partial mutual inductance is shown to be smaller than 0.01 nH/m depending on the relative position of the two elements. The voltage measurement points on the loops are connected by impedance matching coaxial cable to the Gain-Phase-Analyzer so that no influence on the field distribution in the setup is achieved.

Nagel [6] calculates ESL only from the area of the loop, assuming the capacitors current flows closest to its bottom edge due to proximity effect. Calculating loop inductances of thin wires according to Paul [7] with Nagel's proximity assumption provides self inductances of the loop with the capacitors of 76nH for 15mm grid size, 93nH for 22.5mm and 104nH for 27.5mm. As these values are quite accurate, modeling the coupling behaviour is tested with one element at the bottom edge of the capacitor under the proximity assumption (Figure 7).

Figure 8 shows measured data of the setup with the $1\mu\text{F}$ Capacitor and calculated data from the equivalent circuit shown in Figure 3. The resonance frequency is calculated quite accurately by determining the parameters of the equivalent circuit under the proximity assumption. The results provide an approximate value for ESL of 102nH, similar to the expected value of 104nH. But coupling with a mutual inductance of 2.8nH is much to high. Thus, the proximity assumption is admissible for the determination of approximate values of self inductances but not for the determination of mutual inductances.

The simplest way to model the shape of the metalized film roll is to replace the wire at the bottom edge with a single cuboid element with the width, height and length of the metalized film roll. In the case of the $1\mu\text{F}$ capacitor the PEEC method provides the same value (103nH) for the self inductance as under the proximity assumption and a good value for the

mutual inductance of 0.5nH. But compare the measurement in Figure 8 with the cuboid calculation again. There is still a deviation of the calculated resonance frequency from the 540kHz measured: the approximate value for ESL of 103nH is too large.

As with the cuboid ESL is not predicted very accurate, the round corners of the film roll are emulated by 20 elements modeling the roll in detail. In order to properly model the non-uniform current distribution in x-direction aswell, the 20 elements are finer discretized in 4 filaments each, resulting in 80 elements altogether. The detailed modeling approach (20 elements in z-, 4 elements in x-direction) provides exactly the measured self inductance of 91nH and an as accurate value for the mutual inductance. Eighty elements per capacitor are no challenge in terms of computation time and memory requirements. Thus, the demands in calculation time and memory are straightforward and the detailed modeling approach is worthwhile obtaining correct inductance values in real world circuits.

V. CAPACITIVE COUPLING

The coupling capacitance between the primary and the secondary side is strongly dependant on the size of the component which acts as an electrode of the mutual capacitance. Therefore the second resonance is only for the 1μF capacitor within the regarded frequency range. Another thing to consider is, that only the outermost metalized film couples capacitively. With usual film capacitors the outermost film is connected to only one connector of the capacitor. Thus, the outermost film is to be connected to the lower potential in order to avoid capacitive coupling in the circuit [8]. The capacitors under test in this paper have a floating electrode increasing the proof voltage and the outermost film is split into two parts, each connected to one connector of the capacitors. A coupling capacitance C_k is added to the equivalent circuit in Figure 3 modeling the described behaviour. In case of usual capacitors C_k connects one connector with the antenna loop (Figure 9, on the left). In case of capacitors with internal series connection C_k is split into two parts as shown on the right of Figure 9. The determination of accurate values for C_k is straightforward and can be obtained by the PEEC method or even by two

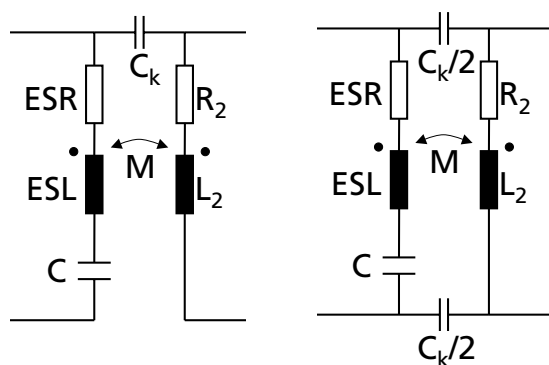


Fig. 9. Adding the coupling capacitance to the equivalent circuit

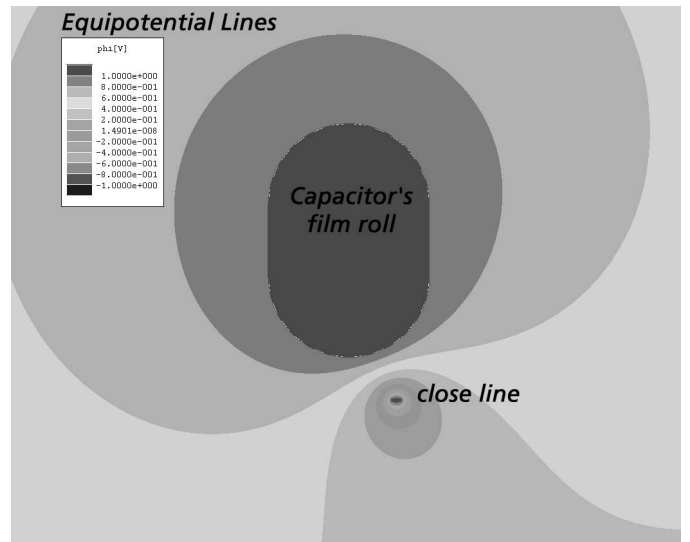


Fig. 10. Determining the coupling capacitance by 2D electrostatic calculation

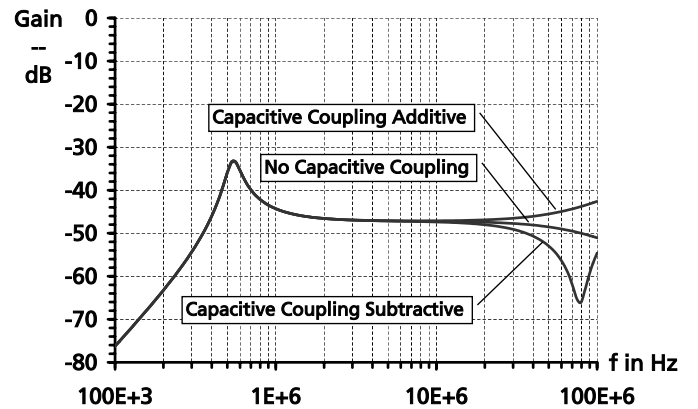


Fig. 11. Depending on the ground connection to the secondary side, more or less voltage is coupled to the antenna loop capacitively from the loop with the 1μF capacitor

dimensional electrostatic field solver (Figure 10).

Depending on the connection of the reference potential to the measurement setup the partial voltage coupled onto the antenna loop capacitively can clearly be evaluated. Figure 11 shows the received voltage with the 1μF capacitor calculated with and without capacitive coupling and different connection of the reference potential. The difference is a few dB at 30MHz increasing up to 20dB at the resonance frequency of 78MHz. Capacitive coupling is rising with frequency and shows considerable values at 30MHz.

A few more calculations with different loop positions in three dimensions are presented in the following in order to proof the accuracy of the detailed modeling approach.

VI. POSITION OF ANTENNA LOOP

The presented modeling approach for the calculation of coupling and parasitic elements including conducting structures and EMI capacitors is validated by comparing measured

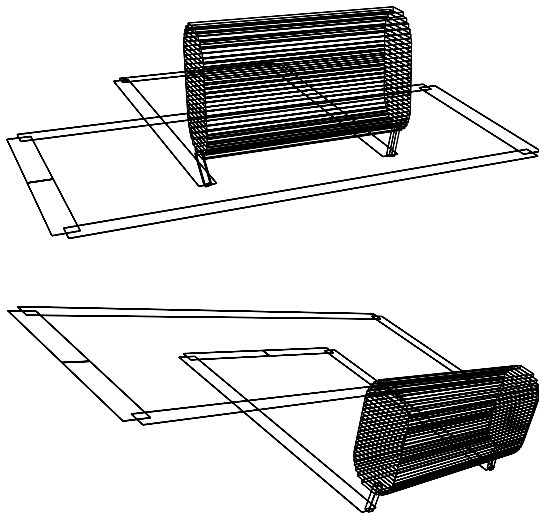


Fig. 12. Models with antenna loop at a level above the level of the connectors to the 330nF capacitor and at two different sides

and calculated data with different positions of the antenna loop. Figure 13 shows measured and calculated gain with the antenna loop at a level above the level of the connectors to the 330nF capacitor and at two different sides. At the end of the regarded frequency range measurement and calculation differ slightly because capacitive coupling is not considered here and the equivalent circuit shown in Figure 3 is used. Up to 30MHz calculations and measurement match perfectly and thus prove the possibility to predict coupling with EMI capacitors and their parasitic elements at the system level of circuits built in three dimensions.

VII. CONCLUSION

With the presented calculations one step towards methodical design of EMI filters including the filter's radio frequency behaviour is done. Parasitic elements of EMI capacitors and coupling to close conductors are calculated using the PEEC method. The approach is verified by experimental results. It provides very accurate parasitic inductances and mutual inductances under the assumption of straight and centered metalized film rolls within the capacitors' housing. 80 elements per capacitor are added to the systems discretization for the field coupling calculation. Thus the demands in calculation time and memory are straightforward and the possibility to simulate field coupling in circuits built in all three dimensions

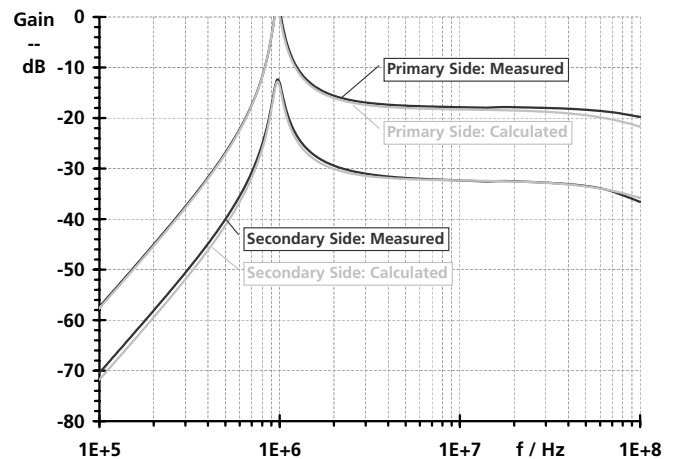


Fig. 13. Measured and calculated data with antenna loop at one side respectively the other side of the 330nF capacitor

including the circuit's components is proven. In particular when miniaturizing power electronic devices the calculated coupling among conductors and components must be taken into account to ensure EMC at the system level. Design of EMI filters will take their radio frequency behaviour into account. Therefore the behaviour of all other parts like filter chokes and housing and coupling among them and conductors have to be investigated in future works.

REFERENCES

- [1] Marco Chiado Caponet, Francesco Profumo, Alberto Tenconi, *EMI Filters Design for Power Electronics*, Power Electronics Specialists Conference, 2002
- [2] Andreas Nagel, R.W. De Doncker, *Systematic Design of EMI Filters for Power Converters*, IEEE Industrial Applications Conference, 2000
- [3] Eckart Hoene et al., *Evaluation and Prediction of Conducted Electromagnetic Interference Generated by High Power Density Inverters*, EPE Conference, Graz, Switzerland, 2001
- [4] André Görisch, *Netzwerkorientierte Modellierung und Simulation elektrischer Verbindungsstrukturen mit der Methode der partiellen Elemente*, Dissertation Otto-von-Guericke-Universität Magdeburg, Cuvillier Verlag, Göttingen, 2002
- [5] Albert E. Ruehli, *Equivalent Circuit Models for Three-Dimensional Multiconductor Systems*, IEEE Transactions on Microwave Theory and Techniques, 1974
- [6] Andreas Nagel, *Leitungsgebundene Störungen in der Leistungselektronik: Entstehung, Ausbreitung und Filterung*, Dissertation RWTH Aachen, Wissenschaftsverlag, Mainz, 1999
- [7] Clayton R. Paul, *Introduction to Electromagnetic Compatibility*, John Wiley and Sons, New York, 1992
- [8] H.Friedeli, *Folienkondensatoren richtig gepolt*, Elektor 2/2004, Elektor-Verlag, S.25, Aachen, 2004